Brain, Behavior, and Immunity 117 (2024) 399–411

Contents lists available at ScienceDirect

Brain Behavior and Immunity

journal homepage: www.elsevier.com/locate/ybrbi

# KCNA2 IgG autoimmunity in neuropsychiatric diseases

Friederike A. Arlt [a,b], Ramona Miske [c], Marie-Luise Machule [a,b], Peter Broegger Christensen [d], Swantje Mindorf [c], Bianca Teegen [e], Kathrin Borowski [e], Maria Buthut [a,b,ai], Rosa Rößling [a,b], Elisa Sánchez-Sendín [a,b], Scott van Hoof [a,b], César Cordero-Gómez [a,b], Isabel Bünger [a,b], Helena Radbruch [f], Andrea Kraft [g], Ilya Ayzenberg [h], Jaqueline Klausewitz [h], Niels Hansen [i], Charles Timäus [i], Peter Körtvelyessy [b,j], Thomas Postert [k], Kirsten Baur-Seack [k], Constanze Rost [k], Robert Brunkhorst [l], Kathrin Doppler [m], Niklas Haigis [n], Gerhard Hamann [o], Albrecht Kunze [p], Alexandra Stützer [p], Matthias Maschke [q], Nico Melzer [r], Felix Rosenow [s,t], Kai Siebenbrodt [s,t], Christian Stenør [u], Martin Dichgans [v,w], Marios K. Georgakis [v], Rong Fang [v], Gabor C. Petzold [x,y], Michael Görtler [j,z], Inga Zerr [aa,ab], Silke Wunderlich [ac], Ivan Mihaljevic [ad], Paul Turko [ae], Marianne Schmidt Ettrup [af], Emilie Buchholz [a,b], Helle Foverskov Rasmussen [a,b], Mahoor Nasouti [a,b], Ivan Talucci [m,ag], Hans M. Maric [ag], Stefan H. Heinemann [ah], Matthias Endres [a,b,ai], DEMDAS study group, Lars Komorowski [c], Harald Prüss [a,b,*]

[a] German Center for Neurodegenerative Diseases (DZNE) Berlin, Berlin, Germany
[b] Department of Neurology and Experimental Neurology, Charité-Universitätsmedizin Berlin, Corporate Member of Freie Universität Berlin, Humboldt-Universität Berlin, Berlin, Germany
[c] Institute for Experimental Immunology, affiliated to EUROIMMUN Medizinische Labordiagnostika AG, Lübeck, Germany
[d] Department of Neurology, Aalborg University Hospital, Aalborg, Denmark
[e] Clinical immunological Laboratory Prof. Stöcker, Groß Grönau, Germany
[f] Department of Neuropathology, Charité-Universitätsmedizin Berlin, Corporate Member of Freie Universität Berlin, Humboldt-Universität Berlin, Berlin, Germany
[g] Department of Neurology, Hospital Martha-Maria, Halle, Germany
[h] Department of Neurology, St Josef-Hospital, Ruhr University Bochum, Bochum, Germany
[i] Department of Psychiatry and Psychotherapy, University Göttingen Medical Center, Göttingen, Germany
[j] German Center for Neurodegenerative Diseases (DZNE) Magdeburg, Magdeburg, Germany
[k] Department of Neurology, St. Vincenz-Krankenhaus Paderborn, Paderborn, Germany
[l] Department of Neurology, University Hospital Aachen, Aachen, Germany
[m] Department of Neurology, University of Würzburg, Würzburg, Germany
[n] Department of Child and Adolescent Psychiatry, Centre for Psychosocial Medicine, University of Heidelberg, Heidelberg, Germany
[o] Department of Neurology and Neurological Rehabilitation, BKH Günzburg, Günzburg, Germany
[p] Department of Neurology, Zentralklinik Bad Berka, Bad Berka, Germany
[q] Department of Neurology, Campus Trier, University of Mainz, Trier, Germany
[r] Department of Neurology, Medical Faculty, Heinrich-Heine-University Düsseldorf, Düsseldorf, Germany
[s] Epilepsy Center Frankfurt Rhine-Main, Department of Neurology, Goethe University Frankfurt, Frankfurt on the Main, Germany
[t] LOEWE Center for Personalized Translational Epilepsy Research (CePTER), Goethe University, Frankfurt, Germany
[u] Department of Neurology, Copenhagen University Hospital, Herlev-Gentofte, Denmark
[v] Institute for Stroke and Dementia Research (ISD), University Hospital, LMU Munich, Munich, Germany
[w] German Center for Neurodegenerative Diseases (DZNE) Munich, Munich, Germany
[x] German Center for Neurodegenerative Diseases (DZNE) Bonn, Bonn, Germany
[y] Division of Vascular Neurology, Department of Neurology, University Hospital Bonn, Bonn, Germany
[z] Department of Neurology, University Hospital, Otto-von-Guericke University Magdeburg, Magdeburg, Germany
[aa] German Center for Neurodegenerative Diseases (DZNE) Göttingen, Göttingen, Germany
[ab] Department of Neurology, University Medical Center Göttingen, Göttingen, Germany
[ac] Department of Neurology, Klinikum rechts der Isar, School of Medicine, Technical University of Munich, Munich, Germany
[ad] Department of Neurology, Klinikum Kassel, Kassel, Germany
[ae] Institute for Integrative Neuroanatomy, Charité-Universitätsmedizin, Berlin, Germany
[af] Department of Pathology, Aalborg University Hospital, Aalborg, Denmark
[ag] Rudolf Virchow Center, Center for Integrative and Translational Bioimaging, University of Würzburg, Würzburg, Germany

* Corresponding author at: Department of Neurology and Experimental Neurology, Charité - Universitätsmedizin Berlin, Charitéplatz 1, 10117 Berlin, Germany.
*E-mail address:* harald.pruess@charite.de (H. Prüss).

https://doi.org/10.1016/j.bbi.2024.01.220
Received 25 August 2023; Received in revised form 4 January 2024; Accepted 25 January 2024
Available online 2 February 2024

[ah] Friedrich Schiller University and Jena University Hospital, Center for Molecular Biomedicine, Department of Biophysics, Jena, Germany
[ai] Berlin Institute of Health at Charité - Universitätsmedizin Berlin, Berlin, Germany

ARTICLE INFO

*Keywords:*
Autoantibody
Kv1.2
KCNA2
Autoimmune dementia
Epilepsy
Autoimmune encephalitis
Immunotherapy

ABSTRACT

*Background:* Autoantibodies against the potassium voltage-gated channel subfamily A member 2 (KCNA2) have been described in a few cases of neuropsychiatric disorders, but their diagnostic and pathophysiological role is currently unknown, imposing challenges to medical practice.
*Design / Methods.:* We retrospectively collected comprehensive clinical and paraclinical data of 35 patients with KCNA2 IgG autoantibodies detected in cell-based and tissue-based assays. Patients' sera and cerebrospinal fluid (CSF) were used for characterization of the antigen, clinical-serological correlations, and determination of IgG subclasses.
*Results:* KCNA2 autoantibody-positive patients (n = 35, median age at disease onset of 65 years, range of 16–83 years, 74 % male) mostly presented with cognitive impairment and/or epileptic seizures but also ataxia, gait disorder and personality changes. Serum autoantibodies belonged to IgG3 and IgG1 subclasses and titers ranged from 1:32 to 1:10,000. KCNA2 IgG was found in the CSF of 8/21 (38 %) patients and in the serum of 4/96 (4.2 %) healthy blood donors. KCNA2 autoantibodies bound to characteristic anatomical areas in the cerebellum and hippocampus of mammalian brain and juxtaparanodal regions of peripheral nerves but reacted exclusively with intracellular epitopes. A subset of four KCNA2 autoantibody-positive patients responded markedly to immunotherapy alongside with conversion to seronegativity, in particular those presenting an autoimmune encephalitis phenotype and receiving early immunotherapy. An available brain biopsy showed strong immune cell invasion. KCNA2 autoantibodies occurred in less than 10 % in association with an underlying tumor.
*Conclusion:* Our data suggest that KCNA2 autoimmunity is clinically heterogeneous. Future studies should determine whether KCNA2 autoantibodies are directly pathogenic or develop secondarily. Early immunotherapy should be considered, in particular if autoantibodies occur in CSF or if clinical or diagnostic findings suggest ongoing inflammation. Suspicious clinical phenotypes include autoimmune encephalitis, atypical dementia, new-onset epilepsy and unexplained epileptic seizures.

## 1. Introduction

Autoantibodies against voltage-gated potassium channel (VGKC) complexes have been considered for a long time in patients with distinct autoimmune diseases of the central and the peripheral nervous system (CNS, PNS) such as limbic encephalitis, late-onset epilepsy, and neuromyotonia (Barber et al., 2000; Buckley et al., 2001; Ik et al., 1997; Shillito et al., 1995; Vincent et al., 2004). However, diagnostic refinements have shown that the majority of patients with VGKC complex antibodies actually had specific autoantibodies against the associated extracellular proteins LGI1 (leucine-rich glioma inactivated 1) and CASPR2 (contactin-associated protein-like 2) (Irani et al., 2010; Lai et al., 2010; Quek et al., 2012). Some patients with VGKC complex antibodies are seronegative for both, LGI1 and CASPR2 antibodies. These autoantibodies were shown to often bind to a cytosolic epitope of various potassium voltage-gated channel subfamily A (KCNA) family member subunits, and the small number of reported patients had a limited immunotherapy response (Lang et al., 2017; van Sonderen et al., 2016).

Only recently, a few patients have been described with autoantibodies exclusively targeting Kv1.2 channels (for brevity, KCNA2 is used in this paper as descriptor of both, the gene and the encoded protein Kv1.2), mainly in the context of autoimmune dementia and cryptogenic epilepsy (Kirschstein et al., 2020; Lang et al., 2017; Scharf et al., 2018; Timäus et al., 2021). KCNA channels are crucial for neuronal and synaptic functioning (Guan et al., 2013, 2007; Johnston et al., 2010; Yellen, 2002). The α subunits of the KCNA family form homo- and heterotetrameric protein complexes, thereby producing tissue- and cell type-specific potassium channels with distinct structural and functional properties (Jan and Jan, 2012). In analogy to epileptic, ataxic and neurodevelopmental disorders resulting from mutations in KCNA2 (Corbett et al., 2016; Döring et al., 2021; Manole et al., 2017; Masnada et al., 2017), relevant pathogenic potential of KCNA2 antibodies for neuropsychiatric diseases appears plausible. However, the functional role of KCNA2 IgGs and the association with distinct clinical phenotypes is currently unknown, thus imposing diagnostic and therapeutic challenges for clinical routine. We therefore aimed to describe the clinical phenotypes, paraclinical findings, and response to immunotherapy in the so far largest cohort of patients with KCNA2 autoimmunity. We further used serum and cerebrospinal fluid (CSF) samples for characterization of the underlying epitopes, determination of autoantibody titers and IgG subclasses, and IgG reactivity to distinct anatomical areas in the mammalian CNS and PNS.

## 2. Materials and methods

### 2.1. Study approval

All human samples and clinical investigations were done according to the Declaration of Helsinki principles. All study participants or their representatives gave written informed consent prior to inclusion into the study. All analyses were approved by the Charité Universitätsmedizin Berlin Ethics Board (#EA1/258/18).

### 2.2. Collection of human specimens and antibody screening

This study included patients with KCNA2 IgGs detected in their serum at a reference laboratory. These patients were either referred to Charité Universitätsmedizin Berlin or recruited through external referrals. Retrospectively, the participating centers collected clinical and paraclinical data, as well as serum and CSF samples, from 35 KCNA2 IgG-seropositive patients. Most patients (n = 30) were identified in clinical routine when treating physicians initiated autoantibody testing based on atypical presentation or features of neuroinflammation (e.g. atypical dementia, new epileptic seizures of unexplained etiology, CSF inflammation, MRI lesions, or rapidly progressing neurological deterioration of unexplained cause). Additional cases (n = 5, patients #30–34) were recruited through systematic autoantibody testing in the prospective multicenter DZNE – mechanisms of Dementia after Stroke (DEMDAS) trial (clinical trials.gov: NCT01334749). Two patient cases (patient #20 and patient #21) have been previously published (Timäus et al., 2021). KCNA2 IgG detection was conducted using a biochip array with acetone-fixed recombinant human embryonic kidney 293 (HEK293) cells separately expressing brain antigens Hu, Yo, Ri, CV2,

PNMA2, ITPR1, Homer 3, CARP VIII, ARHGAP26, ZIC4, DNER/Tr, GAD65, recoverin, GABAB receptor, glycine receptor, DPPX, IgLON5, glutamate receptors (types NMDA, AMPA, mGluR1, mGluR5, GLURD2), LGI1, CASPR2, AQP4, MOG, ATP1A3, NCDN, Flotillin 1/2, KCNA2, AP3B2, Sez6L2, CNTN1, NF155, NF186 or empty vector-transfected HEK293 cells as controls. Anonymized sera of 96 healthy blood donors were used as controls. All samples were aliquoted and stored at −80 °C or −20 °C until first experimental use. Hereafter, samples were stored at + 4 °C for additional experiments thereby avoiding repeated freeze/thaw cycles.

### 2.3. Recombinant expression of KCNA2, KCNA1, and KCNA6 in HEK293 cells

KCNA2, KCNA1, and KCNA6 were transiently expressed in HEK293 cells as previously described (Miske et al., 2023). Briefly, human genomic DNA was extracted from HEK293 cells and used as a template for amplification of the coding sequence of KCNA1, KCNA2 and KCNA6 by polymerase chain reaction (PCR). Respective DNA oligonucleotides were used introducing the given enzyme restriction sites (see Table 1). The amplified PCR fragments were digested with the indicated enzymes and separately ligated with NcoI/XhoI-linearized pTriEx-1 (Merck). KCNA1, KCNA2, and KCNA6 proteins were transiently expressed following PEI-mediated transfection (PEI 25K$^{TM}$), according to manufacturer's instructions (Polysciences Europe). For indirect immunofluorescence assays, cells were grown on coverslips and fixed with acetone or methanol two days after transfection or used for live cell immunofluorescence assays as described in section 2.9.

### 2.4. Animals

All animal procedures were approved by the Landesamt für Gesundheit und Soziales (LaGeSo) Berlin, Germany (approval numbers T-CH 0009/22, G0078/19), and performed in compliance with German and international guidelines for care and humane use of animals. Male C57BL/6 mice were used at an age of 10–12 weeks. For primary dissociated cell cultures, male and female Wild-type (WT) Wistar rat pups or NexCre;Ai9xVGAT Venus mice were humanely sacrificed at postnatal days (P0–P2). All animals were housed in temperature- and humidity-controlled conditions on a 12 h dark and light cycle and always provided with food and water ad libitum.

### 2.5. Primary dissociated cell cultures

Primary dissociated cell cultures were prepared from either WT Wistar rat pups or NexCre;Ai9xVGAT Venus mice as previously described (Turko et al., 2019a, 2019b). In brief, neocortical tissue was excised and then papain-dissociated (1.5 mg/mL; Merck) for 30 min at 37 °C, before trituration in bovine serum albumin (10 mg/ml; Merck). Cells were then counted before resuspension in Neurobasal A medium (supplemented with 1 × B27, 1 × Glutamax, and 100 U/ml Penicillin-Streptomycin; Thermofisher Scientific). Dissociated cells were grown on 12-mm glass coverslips (Roth) previously coated for 1 h with poly-L-lysine hydrobromide (20 μg/ml; Merck), in 24-well cell culture plates (BD Falcon). Cells were typically plated in 20 μl droplets at a density of 2000 cells / μl (total: 4 x $10^4$ cells per coverslip). Cultures were grown in humidified conditions at 37 °C and 5 % $CO_2$ until harvesting at DIV 20–22. WT rat neurons, without fluorescent labeling, were fixed and permeabilized in 100 % methanol for 3 min at −20 °C and stored in phosphate-buffered saline (PBS) at 4 °C until further processing. GABAergic neurons expressing enhanced yellow fluorescent protein (Venus) and glutamatergic neurons expressing tdTomato were used for live cell staining as explained in section 2.9.

### 2.6. IgG purification from serum

IgG purification was adapted from a previously established antibody purification protocol (Kreye et al., 2016). In brief, 200 μl of serum and 200 μl of Protein G Sepharose Beads 4FastFlow Cytiva® (Merck) were incubated in 50 ml PBS overnight at 4 °C. Samples were centrifuged at 4,000 g, supernatant was removed, and the beads were transferred to Bio-Spin® chromatography columns (Bio-Rad), which were previously equilibrated and washed with PBS. IgGs were eluted from the columns using 500 μl elution buffer (0.1 M sodium citrate, pH 2.7, Thermofisher Scientific), and pH-neutralized with 50 μl 1.5 M Tris (pH 8.8). Buffer exchange to PBS was performed using PD-10 columns (Sephadex$^{TM}$ G-25 medium, Sigma-Aldrich). IgGs were sterile filtered, and final concentrations were determined using NanoDrop (Thermofisher Scientific). KCNA2 IgG reactivity was confirmed by cell- and tissue-based immunofluorescence assays on KCNA2-transfected HEK293 cells and murine cerebellum, following the procedures described in section 2.9.

### 2.7. Intrathecal osmotic pump infusion

100 μg of purified IgGs from patient #3 and from a control serum were infused into the right ventricle of two WT mice using osmotic pumps (model 1002, Alzet) over a 14-day period. The pumps were filled 24 h before the surgical implantation, during which the mice were placed in a stereotaxic frame, and a cannula was inserted into the right ventricle at specific coordinates (0.2 mm posterior and ± 1.00 mm lateral from bregma, depth 2.2 mm). The cannula was then connected to a subcutaneously implanted pump. Throughout the 14-day experiment, daily monitoring of the mice was conducted to assess symptoms and weight fluctuations. On day 14, the mice were euthanized, and their brains were dissected, fixed in 4 % paraformaldehyde (PFA) overnight, and then cryoprotected in 30 % sucrose for 2 days prior to freezing and cryosectioning, following the procedures described in section 2.8.

### 2.8. Animal brain and sciatic nerve processing

Unfixed brains and PFA-fixed IgG-infused brains were dissected and frozen in 2-methylbutan. Cryostat-cut 20 μm sections were mounted on

**Table 1**
DNA oligonucleotide sequences for PCR amplification of cDNA fragments of KCNA1, KCNA2 and KCNA6. F: forward primer, R: reverse primer.

| Protein | Restriction sites | DNA oligonucleotide sequence (5'-3') |
|---|---|---|
| KCNA1 | Eco31I (BsaI) XhoI | F: ATTAGGTCTCACATGACGGTGATGTCTGGGGAGAACGTGGA<br>R: TATCTCGAGTTAAACATCGGTCAGTAGCTTGCTCTTATTAACG |
| KCNA2 | NcoI XhoI | F: ATTCCATGGCAGTGGCCACCGGAGACCCAGCAGACGAG<br>R: TATCTCGAGTCAGACATCAGTTAACATTTTGGTAATATTCAC |
| KCNA6 | PagI (BspHI) XhoI | F: ATATCATGAGATCGGAGAAATCCCTTACGCTGGCG<br>R: TATCTCGAGTCAGACCTCCGTGAGCATTCTTTTCTCTG |

glass slides and stored up to seven days prior to tissue-based immunofluorescence. Murine sciatic nerves were dissected and directly fixed in 4 % PFA for 20 min on ice. After washing with PBS, the epineurium was removed using a stereo microscope (Leica EZ4W). The nerves were teased on glass slides, air-dried overnight, and stored at −20 °C up to four weeks until further usage. Prior to staining, teased fibers were post-fixed and permeabilized with 100 % methanol for 2 min at −20 °C and washed with PBS.

### 2.9. Cell- and tissue-based immunofluorescence assays and IgG subclass determination

Indirect immunofluorescence assays were performed as described previously (Kreye et al., 2016; Miske et al., 2023; Prüss, 2021). Assays were conducted using brain tissue cryosections (hippocampus of rat, cerebellum of rat and monkey, and mouse whole brain), mouse sciatic nerve teased fibers, primary neuronal cultures or acetone-fixed recombinant HEK293 cells separately expressing KCNA1, 2, or 6, using empty vector-transfected HEK293 cells as controls. Slides were incubated with PBS-diluted sample at room temperature (RT) for 30 min, washed with PBS-Tween and immersed in PBS-Tween for 5 min. Alternatively, fixed and permeabilized cells or slides with brain or nerve tissue were rinsed with PBS prior to incubation with blocking solution (10 % normal goat serum, 2.5 % bovine serum albumin and 0.1 % Triton-X) for 1 h at RT followed by overnight incubation of serum, CSF and commercial anti-KCNA2 antibody (Neuromab K14/16 final dilution of 1:200) at 4 °C in blocking solution. Further primary antibodies used as controls were anti-KCNA2 antibody (Sigma-Aldrich, SAB1100129-200UL, final dilution 1:1,000), anti-KCNA1 antibody (Chemicon, AB9782, final dilution 1:1,000), and anti-KCNA6 antibody (Sigma-Aldrich, HPA014418-100UL, final dilution 1:200). In the second step, either Alexa488-labelled goat anti-human IgG (Dianova, 109–545-003, final dilution 1:1,000), fluorescein isothiocyanate (FITC)-labelled goat anti-human IgG (EUROIMMUN Medizinische Labordiagnostika AG, undiluted), IgG subclass specific FITC-labelled mouse anti-human IgG (Sigma-Aldrich F0767, F4516, F4641, F9890, final dilution 1:200), Alexa594-labelled goat anti-mouse IgG (Jackson Research 115–585-03, final dilution 1:500), or Cy3-labeled goat anti-rabbit IgG (Dianova, 111–165-045, final dilution 1:400) were incubated at RT for 30 min. After washing with PBS, cell nuclei were visualized by DNA staining with TO-PRO-3 iodide (Thermofisher Scientific, final dilution of 1:2,000) or DAPI (Sigma-Aldrich, final concentration of 0.067 μg/ml). Endpoint titers refer to the last dilution showing visible fluorescence. IgG-infused and PFA-fixed brain cryosections were blocked with blocking solution, stained with Alexa488-labelled goat anti-human IgG (Dianova, 109–545-003, final dilution 1:1,000), and after washing, subsequently stained with commercial anti-KCNA2 antibody (Neuromab K14/16 final dilution 1:200) and secondary Alexa594-labelled goat anti-mouse IgG (Jackson Research 115–585-03, final dilution 1:500).

Live cell assays were performed in KCNA2-overexpressing HEK293 cells and primary hippocampal neuronal cultures. 48 h after transfection (HEK293) and on day 20–22 (neurons) the cells were incubated with sera (dilution 1:300) and CSF (dilution 1:2) for 1 h in cell culture media at 37 °C. After rinsing with PBS, cells were fixed in 4 % PFA for 10 min at room temperature and washed with PBS. Cells were blocked with blocking solution without Triton-X and secondary antibodies against human pan-IgG (Dianova, 109–545-003, final dilution 1:1,000 or Thermofisher Scientific a21445, final dilution 1:500) were applied overnight at 4 °C. Imaging was conducted within 48 h after staining using widefield and confocal microscopes. Images were processed using NIH Image J software Version 2.9.0 (Bethesda, MD).

For neutralization assays, selected sera (final dilution 1:400) were incubated with KCNA2-HEK293 cell extracts (final dilution 1:10) in PBS-Tween using empty-vector-transfected HEK293 (final dilution 1:10) as controls. Sections and cells were sequentially stained with commercial KCNA2 antibodies (Neuromab K14/16).

### 2.10. Western blotting

Western blotting using patients' sera was performed as previously described (Miske et al., 2021). In brief, HEK293 cell extracts containing the overexpressed KCNA2 or empty vector transfected HEK293 control extracts were incubated with NuPage LDS sample buffer (Thermofisher Scientific) followed by SDS-PAGE (NuPAGE, Thermofisher Scientific). Separated proteins were electrotransferred onto a nitrocellulose membrane by tank blotting with transfer buffer (Thermofisher Scientific) according to the manufacturer's instructions. The membranes were blocked with 1:5 diluted sample buffer (EUROIMMUN) for 15 min and incubated with the patient sera (dilution of 1:200). After washing with Universal Blot Buffer (EUROIMMUN), the membranes were incubated with anti-human-IgG-AP (EUROIMMUN, final dilution 1:10) for 30 min, washed, and stained with NBT/BCIP substrate (EUROIMMUN).

### 2.11. Histopathological analyses

PFA-fixed and paraffin embedded tissue of patient #25 was cut in 3–4 μm sections. Routine histological staining (H&E, Luxol fast blue) was performed according to standard procedures. Immunohistochemical staining was performed on Ventana Benchmark Ultra (Roche Diagnostics, Switzerland) or Dako Omnis autostainer (Agilent, USA) with standard antigen retrieval methods. The following primary antibodies were used against GFAP (DAKO – M0761, clone 6F2, final dilution 1:250), Ki67 (DAKO – M7240, clone MIB1, 1:200), CD3 (Leica – NCL-L-CD3-565, clone LN10, 1:100), CD4 (Cell Marque – 104R-15, clone SP35, 1:50), CD8 (DAKO – M7103, clone C8/114B, 1:300), CD20 (DAKO – M075501, clone L26, 1:400), CD68 (DAKO – M087601, clone PG-M1, 1:50), and CD163 (Cell Marque / 163 M−16, clone MRQ-26, 1:40). Briefly, primary antibodies were applied and developed using the Ventana OptiView (Roche Diagnostics, Switzerland) or Dako EnVision FLEX (Agilent). Sections were counterstained with hematoxylin, dehydrated in a graded alcohol and xylene series, mounted and coverslipped. Immunohistochemistry sections were evaluated by at least one board-certified neuropathologist. To biologically validate all immunohistochemistry stainings, control tissues harboring or lacking the expected antigens were used on the slides. Sections were scanned with an Aperio GT 450 (Leica Biosystems, Germany) and images of regions of interest were taken Aperio Image Scope (Leica). All images are uploaded on zenodo (https://doi.org/10.5281/zenodo.8272855).

### 2.12. Statistical analysis and data visualization

All statistical analyses were performed using SPSS Statistics Version 28.0.0 (IBM, Armonk, NY). Two-sided Fisher's exact tests were used for comparisons of categorial variables. Crude logistic regression analysis was used to test for associations of KCNA2 IgG titers with main diagnoses and symptoms as well as diagnostic findings. Statistical significance was set at $p < 0.05$. Data visualization was conducted in Prism Version 9.4.1 (GraphPad Software, San Diego, CA) and Inkscape Version 1.2.1 (Inkscape Project. 2020, available at https://inkscape.org).

## 3. Results

### 3.1. KCNA2 IgG autoantibodies in patients and healthy controls

Between April 2016 and April 2022, we retrospectively collected clinical and paraclinical data of 35 consecutive patients seropositive for KCNA2 IgG autoantibodies. Patients' median age at disease onset was 65 years (IQR 55–72), and 74.3 % were male. KCNA2 IgG was detected in cell-based assays (CBAs) and titers ranged from 1:32 to 1:10,000 in serum (median 1:1,000) (Fig. 1A). CSF was collected from 29 patients (82.9 %) of the cohort. Of these, 21 CSF samples (60 %) were submitted for KCNA2 IgG testing at the discretion of the treating physicians, and among those, 8 tested positive (Fig. 1A). In a control population of 96

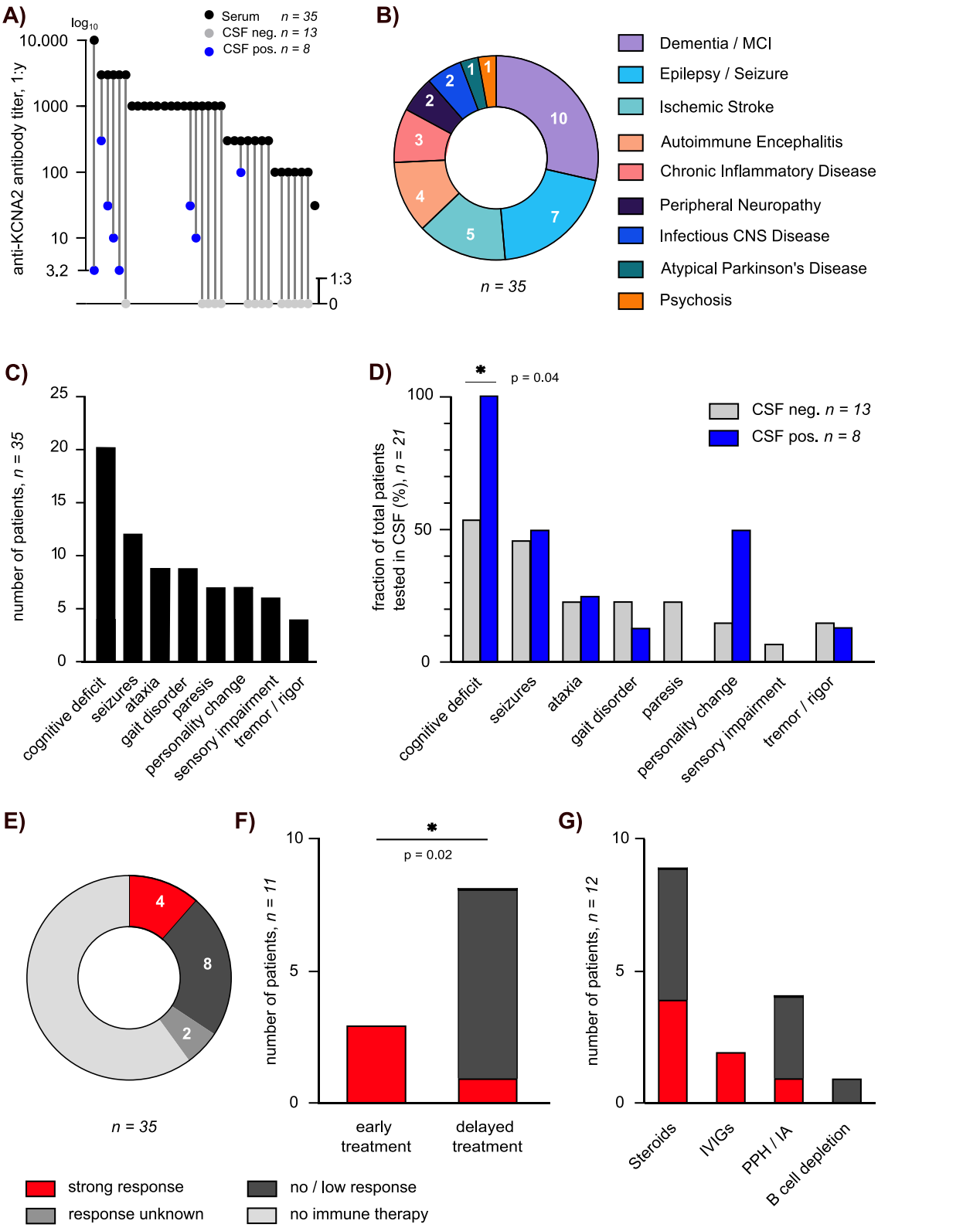


**Fig. 1. Clinical and paraclinical features of KCNA2 IgG seropositive patients** A) KCNA2 antibody titers in serum (black, n = 35) and CSF (positive = blue [n = 8], negative = grey [n = 13]), paired samples per patient are connected with a line. B) The clinical spectrum of KNCA2 IgG-associated disease was heterogeneous with dementia / MCI, epilepsy / seizure, and ischemic stroke being the leading diagnoses. C) Main symptoms at disease onset of patients with KCNA2 IgGs in serum. D) In patients with KCNA2 IgGs also in CSF (n = 8), cognitive impairment was more frequent than in CSF-negative patients (n = 13), while other main symptoms were not significantly different. E) Immunotherapy was applied in 14/35 patients, showing a strong response (red) in n = 4, no/low response (dark grey) in n = 8 and unknown response (grey) in n = 2. F) Early immunotherapy (starting within 6 months of symptom onset) showed higher response rates compared to delayed treatment (≥6 months). G) Response to immunotherapy in correlation with administered medication (available for n = 12 patients). All correlations were calculated using Fisher's exact test, asterisks indicate statistical significance with $p < 0.05$. (For interpretation of the references to colour in this figure legend, the reader is referred to the web version of this article.)

healthy blood donors, KCNA2 IgG was detected in 4 serum samples (4.2 %). Autoantibody titers were similar to patients (median 1:1,000). Considering the autoantibodies tested here, only two patients had additional autoantibodies: Patient #19 had anti-AP3B2 (titer 1:32) and patient #30 anti-NMDAR IgM (1:1,000) autoantibodies in serum.

### 3.2. Serum KCNA2 IgGs are detected in patients with heterogeneous clinical phenotypes

The most common clinical diagnoses in patients with KCNA2 IgG were dementia or mild cognitive impairment (MCI) (n = 10), and epilepsy or first epileptic seizure (n = 7), together accounting for 47.6 % of the cohort (Fig. 1B). In line with the primary diagnoses, main symptoms at disease onset were cognitive impairment (n = 20) and epileptic seizures (n = 12) followed by gait disorder (n = 9) and ataxia (n = 9) (Fig. 1C). Serum KCNA2 IgGs were further identified in patients with acute ischemic stroke (n = 5), of whom 80 % had cognitive impairment in the acute stroke phase, as assessed with pathological MoCA (Montreal Cognitive Assessment) testing. 2/3 available follow-up MoCA tests remained pathological six months after stroke.

Further diagnoses included definite (n = 4) or possible (n = 2) autoimmune encephalitis (AIE) showing subacute or acute onset of status epilepticus (patient #23), headache with dizziness and epileptic seizures (patient #25), cognitive decline and change of mood and behavior (patient #21), and brainstem syndrome with epileptic seizures (patient #12). Two patients with clinical features of possible AIE showed hippocampal swelling on brain MRI (patient #10) or epileptic seizures with verbal memory deficits and pleocytosis (patient #35). In these 6 cases (17.1 %) with the clinical diagnosis of AIE, no other known anti-neuronal antibodies beyond KCNA2 were initially detected, only 2 showed KCNA2 IgG in CSF, assessed by CBA. A subset of patients complained mainly of sensory impairment and neuropathic pain, and 2 patients had infectious CNS disease (Fig. 1B). Paresis was evident in 7 cases, and 7 patients displayed personality changes, mainly in the context of MCI or dementia (Fig. 1C). No association of predominant clinical manifestation with KCNA2 autoantibody titers in serum or CSF was seen (data not shown).

### 3.3. KCNA2 IgG positivity in CSF is associated with cognitive impairment

Next, we analyzed whether the presence of KCNA2 IgGs in CSF, resulting from intrathecal synthesis and/or blood–brain barrier impairment, may be associated with distinct clinical phenotypes (Fig. 1D). Indeed, all 8/8 CSF-positive patients had cognitive impairment compared to only 7/13 patients with KCNA2 IgG detected in serum only (p = 0.046, two-sided Fisher's exact test). No difference was observed in other clinical symptoms between CSF-positive and CSF-negative patients (Fig. 1D). In addition, the presence of KCNA2 IgGs in CSF did not correlate with other pathological abnormalities in MRI, CSF and EEG (see Table 2) in our cohort (data not shown).

### 3.4. Early immunotherapy may be beneficial

The majority of patients (21/35) did not receive immunotherapy, likely related to the previously uncharacterized potential role of KCNA2 autoantibodies. Of the remaining 14 patients who received immunotherapy, information on outcomes was available for 12 patients. A strong treatment response with complete or nearly complete remission of symptoms following immunotherapy was observed in 4/12 patients (Fig. 1E), 3 of whom were diagnosed with AIE. All 3 patients who received early immunotherapy within six months of symptom onset showed extensive clinical remission (Fig. 1F) and lost KCNA2 IgG seropositivity in follow-up sera (data not shown). In contrast, patients with long-lasting disease did not show a clear benefit from immunotherapy (Fig. 1F) even if escalated to plasmapheresis or B cell depletion (Fig. 1G). Among the non-responders (5/5), KCNA2 autoantibodies remained detectable at follow-up (data not shown), and these patients exhibited global brain atrophy on MRI (Fig. 2G-I). For detailed clinical and paraclinical data on each patient refer to Supplementary Table 1.

**Table 2**
Summarized diagnostic findings of KCNA2 IgG seropositive patients. * Including temporal / hippocampal atrophy and T2 hyperintensities. MRI: magnetic resonance imaging; CSF: cerebrospinal fluid; EEG: electroencephalogram, PET-CT: positron emission tomography and computed tomography. n (%) total numbers and percentage of total (n = 35).

| | |
|---|---|
| **MRI, n (%)** | 33 (94.2) |
| MRI normal | 2 |
| Pathological MRI | 31 |
| Global atrophy | 13 |
| Specific atrophy | 8 |
| Hippocampal / temporal anomalies* | 10 |
| White matter lesions | 11 |
| Stroke (acute, subacute, chronic) | 7 |
| Any inflammatory lesion | 4 |
| **CSF, n (%)** | 29 (82.9) |
| CSF normal | 13 |
| Pathological CSF | 16 |
| Pleocytosis | 7 |
| Intrathecal antibody synthesis | 9 |
| Blood-brain-barrier impairment | 8 |
| **EEG, n (%)** | 18 (51.4) |
| EEG normal | 9 |
| Pathological EEG | 9 |
| Diffuse brain dysfunction / encephalopathy | 5 |
| Epileptic signals / irregular slowing | 5 |
| **PET-CT, n (%)** | 4 (11.4) |
| PET-CT normal | 0 |
| Pathological PET-CT | 4 |
| cerebral hypometabolism | 3 |
| cerebral hypermetabolism | 1 |

### 3.5. Structural brain changes and signs of inflammation

Brain MRI was performed in 97.1 % of patients (n = 33) and showed pathological changes in almost all of them (n = 31) (Table 2). In line with the frequent cognitive deficits, the most predominant finding was generalized cerebral atrophy in 13/33 patients and localized atrophy in 8/33 patients (Table 1, Supplementary Table 1, Fig. 2G-I). 10/33 patients showed hippocampal or temporal lesions and/or atrophy (Table 2, Fig. 2A-B). Bi-temporal T2 hyperintensities and hippocampal swelling supported the diagnosis of definite or possible AIE in 2 patients (Fig. 2A-B). Additional MRI findings were irregular appearance of right precentral gyrus, acute, subacute, or chronic stroke lesions as potential correlates of epileptic seizures, as well as white matter lesions, and multiple sclerosis-like inflammatory lesions (Table 2, Fig. 2C-F). FDG-PET-CT scans displayed hippocampal hypermetabolism in a case of AIE (patient #25) and local hypometabolism in dementia patients (patients #1 and #6) (Fig. 2J-L).

CSF investigation was conducted in 29/35 patients (82.9 %) and revealed inflammatory pathological changes in 16/29 cases (55 %). These changes included pleocytosis in 7/29 patients, blood–brain barrier impairment in 8/29 patients, and intrathecal antibody synthesis measured through autoantibody index and oligoclonal bands in 9/29 cases (Table 2). 9/18 patients showed pathological changes in EEGs, 5 had interictal epileptiform signals or irregular slowing and 5 showed diffuse brain dysfunction or encephalopathy (Table 2). One patient received a temporal lobe biopsy to rule out a malignant disease. Here, a lymphoplasmacellular infiltration with perivascular cuffing in the white matter was visible with highly activated microglia (CD68 + ) (Fig. 2M-Q). The lymphocytes in the parenchyma were diffusely infiltrating CD3 + T cells and small clusters of CD20 + B cells (Fig. 2P-T, https://doi.

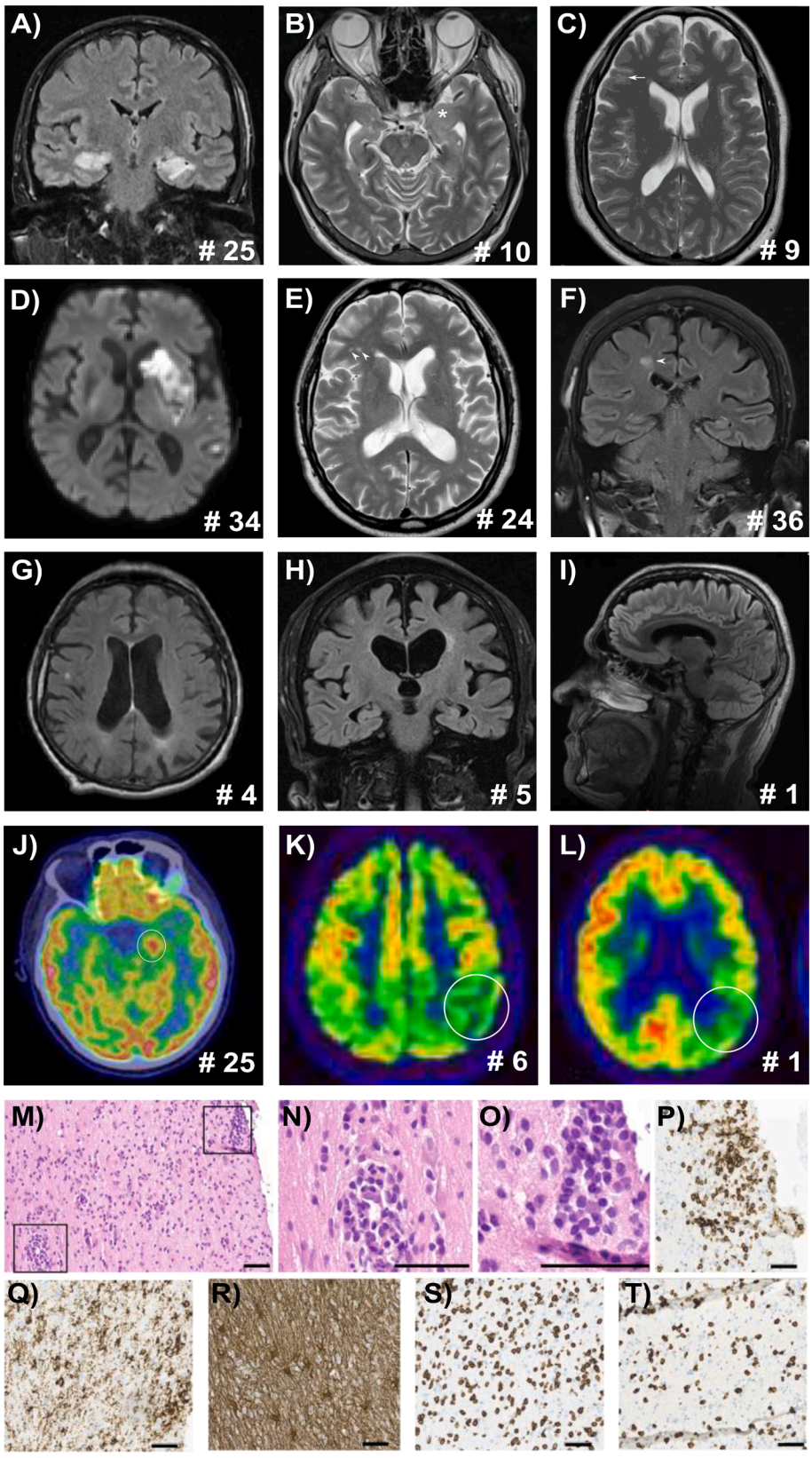


*(caption on next page)*

**Fig. 2. MRI and PET-CT imaging and brain histopathology.** A) T2 FLAIR coronal image of patient #25 showing bitemporal T2 hyperintensities. B) T2 axial image of patient #10 showing left hippocampal swelling (asterisk). C) T2 axial image of patient #9 showing irregular appearance of right precentral gyrus (arrow). D) Diffusion-weighted image of patient #34 showing ischemic infarction. E) T2 axial image of patient #24 showing T2 hyperintensities (arrowheads). F) T2 coronal image of patient #36 showing T2 periventricular hyperintensity (arrowhead). G-I) Examples of global atrophy seen in G) T2 FLAIR axial image of patient #4, H) T2 TIRM dark fluid coronal image of patient #5, and I) T2 FLAIR sagittal image of patient #1. J) Cerebral PET-CT axial image of patient #25 showing left hippocampal hypermetabolism (circle). K) Cerebral PET-CT axial images of patient #1 and L) patient #6 show local hypometabolism (circles). M–Q) Histopathological images of right temporal brain biopsy of patient #25 taken 3 months after symptom onset: H&E staining (M–O) showing perivascular (N) and interstitial (O) infiltrations of lymphocytes and plasma cells in the white matter (N and O zoom ins are marked with black box in M). Immunohistochemistry showing clusters of $CD20^{+}$ B cells (P) in the parenchyma with highly activated microglia (CD68) (Q) and astrogliosis (GFAP) (R).

org/10.5281/zenodo.8272855).

### 3.6. KCNA2 IgGs bind to differentially located epitopes in the CNS and PNS

To determine the epitope locations of KCNA2 IgGs and to test for reactivity in tissue-based assays, available sera and CSF were screened on mammalian brain sections, sciatic nerve teased fibers, and rat primary hippocampal neurons. The KCNA2 tissue expression is highest at the axon initial segment (AIS) of Purkinje cells, in the molecular layer of the hippocampus, and in the juxtaparanodal areas of peripheral nerves, a pattern confirmed with antigen neutralization assays and co-labeling with a commercial KCNA2 positive control antibody, which targets an intracellular part of the protein (Fig. 3E-H,J-L,M–N,red inserts in overlays). Of the human samples, 18/34 sera and 2/8 CSF showed the typical KCNA2 AIS binding pattern of Purkinje neurons in mouse (Fig. 3A), rat (Fig. 3B), or monkey (Fig. 3C) cerebellum. Staining of the hippocampal molecular layer was present in 12/34 sera and 3/8 CSF samples (Fig. 3D). Both patterns disappeared upon HEK293 KCNA2 adsorption (Fig. 3E-H). None of the KCNA2 IgG-positive sera from healthy blood donors showed reactivity in tissue-based brain assays but 2/4 bound to primary hippocampal neurons.

Following the characteristic KCNA2 expression pattern in the PNS, 7/28 sera and 3/8 CSF bound to the juxtaparanodal region of sciatic nerve teased fibers (Fig. 3I-K), thus showing less frequent binding to PNS structures compared to hippocampus and cerebellum. Binding to methanol-fixed primary hippocampal neurons was particularly strong along the main axon and less intense at the dendrites in 21/28 sera and 3/7 CSFs (Fig. 3L-N). No statistically significant associations of tissue or neuron reactivity with main clinical symptoms were evident (data not shown). Cross-reactivity to the closely related potassium channel family members KCNA1 and KCNA6 with similar tissue-reactivity patterns was tested in CBAs. One patient (#12) with immunotherapy-responsive encephalitis showed additional IgG antibodies against KCNA1, while all other tested samples were non-reactive (Fig. 3O). A summary of serum and CSF reactivities in cell- and tissue-based assays is given in Table 3.

### 3.7. In vivo intracellular KCNA2 IgG binding with linear and conformational epitopes

Autoantibody-positive patient samples lacked binding to primary hippocampal neurons (Fig. 3P) and KCNA2-overexpressing HEK cells in live cell assays (Fig. 3Q). This suggests that the human KCNA2 autoantibodies do not recognize neuronal surfaces but instead target an intracellular epitope. Indeed, only after fixation and permeabilization of neurons and KCNA2-transfected HEK293 cells, human samples showed strong binding similar to the KCNA2 commercial antibody (as shown in Fig. 3F and 3G). Binding of 3/4 patients' IgGs to the AIS of Purkinje cells was however visible after intrathecal application into a WT mouse, indicating that the KCNA2 IgGs do reach their targets *in vivo* (Fig. 3R). However, no reactivity was visible in the hippocampal molecular layer after intrathecal application, and no obvious phenotype was evident in the infused animals after 14 days. 3/3 control IgG preparation from sera without KCNA2 antibodies did not show reactivity after intrathecal infusion (Fig. 3S). In a first attempt to better characterize the intracellular epitope, human samples were probed on KCNA2-overexpressing HEK293 cell lysates in Western blots (Fig. 3T). Binding to linearized protein epitopes was detected with 15/29 sera. In contrast, 14/29 sera were non-reactive suggesting that they require a conformational epitope for KCNA2 autoantibody binding. Classifying patient samples as binding to linear versus conformational epitopes did not correlate with main symptoms or diagnoses (data not shown). For detailed data on each patient's serum and CSF reactivity in indirect immunofluorescence assays, Western blots, and KCNA1/KCNA6 CBAs refer to Supplementary Table 2.

### 3.8. KCNA2 IgGs are mainly of IgG1 and IgG3 subclasses

To better estimate the potential IgG subclass-dependent contribution to pathology, we next determined the IgG subclasses of available sera (Fig. 4A-B). IgG3 and IgG1 were the dominant subclasses, either isolated (IgG1 only 8/22, IgG3 only 9/22) or combined (IgG1&IgG3 4/22, IgG1&IgG2&IgG3 1/22) (Fig. 4A-B), both being potent complement activators. None of the examined sera displayed IgG4 reactivity (Fig. 4A-B). We did not detect a correlation of IgG subclasses with clinical presentations (data not shown). Patients with an AIE-related phenotype displayed IgG1 and IgG3 subclasses, similar to the KCNA2 autoantibody-positive healthy blood donors (data not shown). Interestingly, in the majority of patients where KCNA2 autoantibodies were identified in both serum and CSF, the serum autoantibodies belonged to the IgG1 subclass. Conversely, patients who tested negative for CSF autoantibodies primarily exhibited IgG3 autoantibodies in their serum ($p = 0.04$, Fig. 4C).

## 4. Discussion

In this study, we characterized the clinical spectrum and paraclinical findings of a large cohort of patients with KCNA2 IgG autoantibodies. Most patients presented with cognitive impairment and/or epileptic seizures, but also ataxia and gait disorder occurred frequently. KCNA2 autoantibodies bound to the characteristic anatomical areas in the mammalian brain, such as Purkinje cells, hippocampal neurons, and peripheral nerves but reacted exclusively with intracellular epitopes. Intrathecal IgG infusion into a WT mouse, however, revealed intracellular autoantibody binding *in vivo*. Several KCNA2 autoantibody-positive patients markedly responded to immunotherapy, and one available brain biopsy demonstrated strong immune cell invasion. KCNA2 autoantibodies occurred in less than 10 % as a potentially paraneoplastic disease associated with an underlying tumor.

The clinical phenotype observed in our study is in line with the few previous descriptions of KCNA2 autoimmunity (Timäues et al 2021, Kirschstein et al., 2020) and very similar to clinical manifestations of KCNA2-related genetic diseases (Döring et al., 2021, Masnada et al., 2017). A subset of patients presented with sensory impairment and chronic neuropathic pain as previously described for VGKC-seropositive patients (Klein et al 2012).

The lack of functional experiments using patient-derived polyclonal or recombinant monoclonal KCNA2 autoantibodies currently prevents the demonstration of the antibody pathogenicity. On the one hand, the intracellular epitope in all patients does not suggest easy access to the antigen and, in the traditional view, no primary pathogenicity of KCNA2 antibodies. On the other hand, KCNA2 autoantibodies did reach their

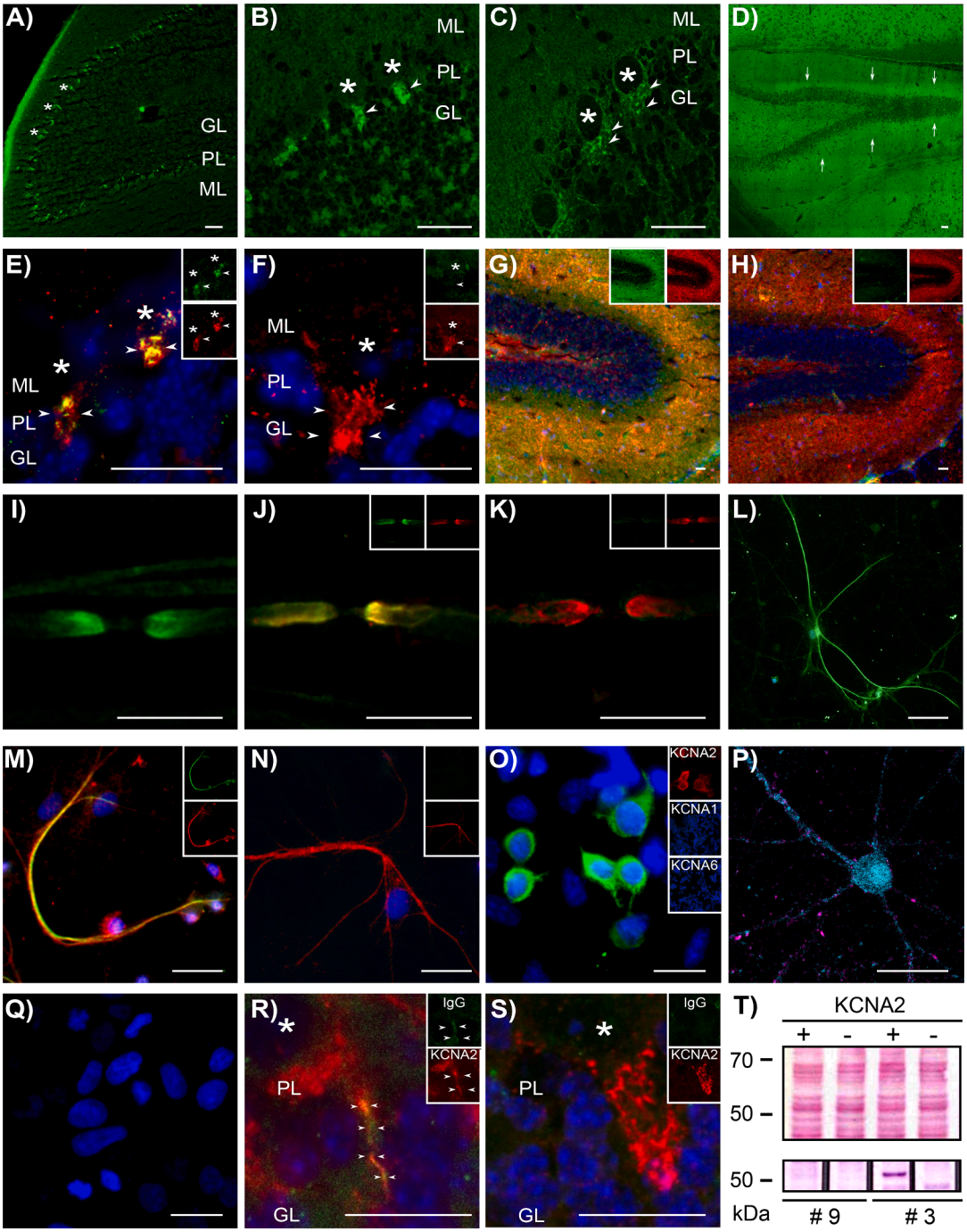


**Fig. 3. KCNA2 IgG immunofluorescence and western blot studies using serum and CSF.** A-S) Representative images of indirect immunofluorescence demonstrating sera staining on mammalian tissues including neutralization assays with HEK293 control extracts and HEK293 KCNA2 extracts, on HEK293 cell-based assays, and after intrathecal IgG infusion (human IgGs in green, commercial KCNA2 antibody in red). Serum showing the characteristic KCNA2 Pinceau pattern on axon initial segments (AIS) of Purkinje cells (arrowhead) on (A) mouse cerebellum, (B) rat cerebellum, and (C) monkey cerebellum (asterisks indicate Purkinje cell soma). D) Serum showing the typical linear KCNA2 binding on molecular layer of mouse hippocampus (arrows). E-H) Sequential staining of serum and a commercial KCNA2 antibody showing signal overlay after preincubation with HEK293 control extract (E&G), while the serum signal is fully neutralized after preincubation with KCNA2 HEK293 extract (F&H). I-K) Likewise, serum showing typical KCNA2 juxtaparanodal binding on murine sciatic nerve teased fiber, which was not neutralized with control (J) but with KCNA2 protein extract (K). L-N) Serum showing typical KCNA2 staining of main axon and less intense of dendrites in primary hippocampal neurons, not neutralized with control (M) but with KCNA2 protein extract (N). O) Serum shows strong reactivity against KCNA2- and no reactivity against KCNA1- and KCNA6-transfected HEK293 cells (KCNA2 positive control shown in red). P) Live primary hippocampal neuron staining shows no reactivity of tested serum (absence of green fluorescence). Q) Live KCNA2-transfected HEK293 cell staining shows no reactivity of tested sera or CSF. R-S) After intrathecal infusion, patient's #3 purified IgGs (R) but not purified control IgGs (S) strongly bound with the typical KCNA2 Pinceau pattern on AIS of Purkinje cell (arrowheads, asterisk indicates Purkinje cell soma). T) Western blot of sera on HEK293 cell lysate transfected with full length KCNA2 (+) and untransfected control HEK293 cell lysate (-) (Ponceau S staining [top] and western blot [bottom]). Representative image of patient #3 showing KCNA2 band at 57 kDa, while patient #9 shows no binding. GL: granular layer, ML: molecular layer, PL: Purkinje cell layer. Scale bar in A-K: 20 μm. (For interpretation of the references to colour in this figure legend, the reader is referred to the web version of this article.)

**Table 3**
Indirect immunofluorescence assays and full-length western blots in KCNA2 IgG seropositive patients. AIS: axon initial segment, HEK: human embryonic kidney cells, KCNA2: voltage-gated potassium channel subfamily A member 2, KCNA1: voltage-gated potassium channel subfamily A member 1, KCNA6: voltage-gated potassium channel subfamily A member 6 CBA: cell-based assay.

| Indirect immunofluorescence with serum | positive / tested |
|---|---|
| AIS pattern on Purkinje cells on brain | 18 / 34 |
| Molecular layer of hippocampus on brain | 12 / 34 |
| Juxtaparanodal pattern on sciatic nerve | 7 / 28 |
| Primary hippocampal neurons | 21 / 28 |
| Live cell hippocampal neurons | 0 / 28 |
| Live cell HEK293 KCNA2 | 0 / 28 |
| HEK293 KCNA1 CBA | 1 / 29 |
| HEK293 KCNA6 CBA | 0 / 29 |
| **Indirect immunofluorescence with CSF** | positive / tested |
| AIS on Purkinje cells on brain | 2 / 8 |
| Molecular layer of hippocampus on brain | 3 / 8 |
| Juxtaparanodal pattern on sciatic nerve | 3 / 8 |
| Primary hippocampal neurons | 3 / 7 |
| Live cell hippocampal neurons | 0 / 7 |
| Live cell HEK293 KCNA2 | 0 / 8 |
| HEK293 KCNA1 CBA | 0 / 7 |
| HEK293 KCNA6 CBA | 0 / 7 |
| **Full-length western blot in serum** | 15 / 29 |

intracellular target also *in vivo* after intrathecal IgG administration. In addition, KCNA2 seropositivity was observed in six patients with otherwise autoantibody-negative definite or suspected AIE and associated with immune cell infiltrates in one available brain biopsy. In addition, clear clinical improvement was observed in 4/35 cases, mainly where immunotherapy was not delayed.

A clear benefit of immunotherapy is difficult to measure in primary neurodegenerative processes because slower progression or stabilization are usually not considered as responsiveness. It seems likely that immunotherapy-responsiveness could be even higher in this and previous cohorts if more patients had received treatment early, in particular before signs of neurodegeneration developed in MRI or CSF. Previous work showed that anti-neuronal antibodies are relatively frequent in patients with neurodegenerative disorders, in particular in atypical cases (Giannoccaro et al., 2021). This further supports the notion that autoantibodies are not only bystanders of neurodegeneration, but may themselves induce or reinforce neurodegenerative cascades such as seen in patients with IgLON5 disease (Gelpi et al., 2016; Landa et al., 2020).

Better outcome with early immunotherapy has become a common principle in autoantibody-associated diseases of the brain (Flanagan et al., 2010; Grüter et al., 2023; Titulaer et al., 2013). Moreover, there is – in addition to our *in vivo* findings for KCNA2 autoantibodies – increasing evidence that autoantibodies against intracellular epitopes may reach their target, for example via Fc receptor-mediated internalization (Bünger et al., 2023; Rocchi et al., 2019), and thus cause low-level 'smoldering' autoimmunity (Prüss, 2021).

The here observed KCNA2 autoreactivity shares many features with autoantibodies against the intracellular antigen glial fibrillary acidic protein (GFAP). In fact, GFAP autoantibodies are not only associated with a relatively common form of an immunotherapy-responsive autoimmune encephalomyelitis (Dubey et al., 2018; Fang et al., 2016; Flanagan et al., 2017), but were also frequently detected in patients with cognitive decline and dementia (Barthel et al., 2023; Long et al., 2018). Although both, GFAP and KCNA2 along with many other autoantibodies were detected in ~ 1 % of more than 2000 healthy controls (Daguano Gastaldi et al., 2023), it is well accepted that GFAP autoimmunity, in particular CSF positivity, is a useful biomarker in the appropriate clinical context to select patients that can benefit from immunotherapy. Likewise, 17 % of KCNA2 IgG-seropositive patients in this study presented with AIE that was not explained otherwise. The predominance of IgG3 and IgG1 subclasses as potent complement activating autoantibodies further suggest a potential role for KCNA2 autoreactivity. Whether KCNA2 autoantibodies can be equally useful biomarkers in

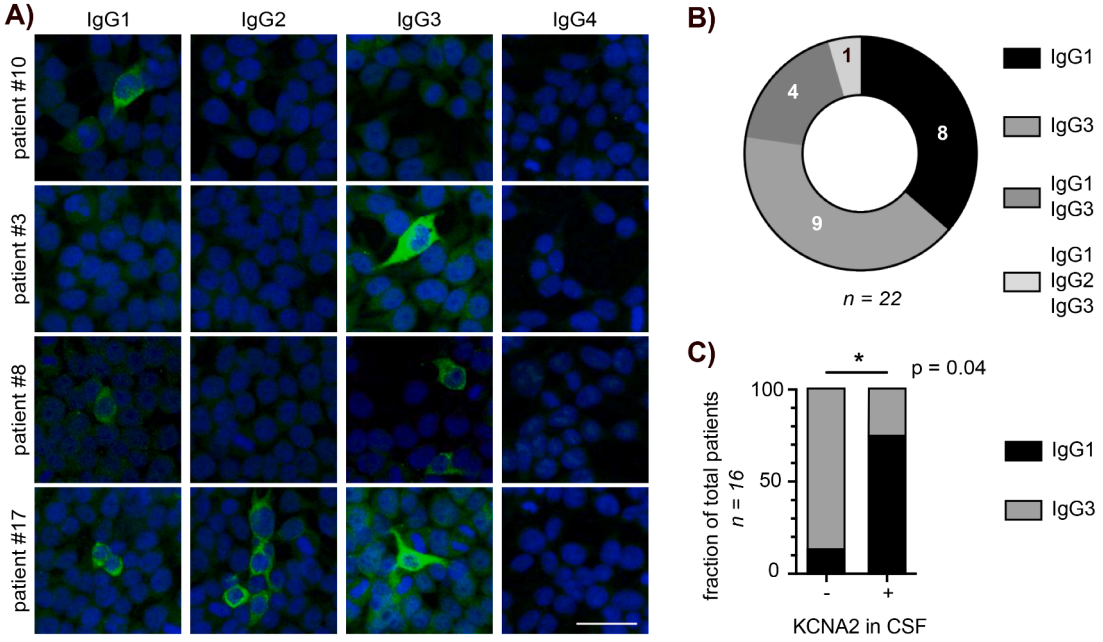


**Fig. 4. IgG subclass determination of KCNA2 IgG-positive sera.** A) IgG subclass determination via indirect immunofluorescence of KCNA2-transfected HEK293 cells. Representative pictures displaying reactivity against IgG1 only (patient #10), IgG3 only (#3), IgG1 and IgG3 (#8) and IgG1, IgG2 and IgG3 (#17). No sample reacted against IgG4. Scale bar: 50 μm. B) Distribution of IgG subclasses for all serum samples. C) The absence of KCNA2 IgGs in CSF (-) is associated with predominant serum IgG3, while the presence of KCNA2 IgGs in CSF (+) is associated with serum IgG1 ($p = 0.04$).

clinical routine for earlier disease detection and treatment decisions, will require analyses of further cases in the future.

The value of autoantibody detection for disease specificity is often higher when assessing CSF autoantibody levels (Kunchok et al., 2019; McKeon et al., 2020; Prüss, 2021). In the present study, CSF KCNA2 autoantibodies were associated with cognitive impairment, and dementia was the leading diagnosis in many patients. Notably, only one patient's CSF with a particularly high CSF titer of 1:100 tested positive in all applied assays consistently suggesting a broader polyclonal repertoire with high-affine or more abundant antibodies. Interestingly, this patient #23 presented with status epilepticus, cognitive impairment, pleocytosis and intrathecal antibody production, similar to the patient published by Kirschstein et al. (2020). The patient was diagnosed with AIE and responded well to several cycles of methylprednisolone therapy. KCNA2 autoantibodies were of IgG1 subclass and tested negative on follow-up, in line with clinical remission. Experimental work in rats demonstrated that human KCNA2 IgG could alter long-term potentiation and synaptic transmission in Schaffer-Collteral-CA1 synapses (Kirschstein et al., 2020). Future studies will clarify whether KCNA2 autoantibodies are directly involved in this process and may thus define – or at least aggravate – a novel subtype of autoimmune dementia.

## 5. Limitations

One limitation of our study is the retrospective acquisition of clinical data and lack of standardized diagnostic tests across participating centers, for example for seizure frequency monitoring or neuropsychological assessments. Frequently, only cross-sectional data were available. Due to the limited amounts of patients' biomaterial, in particular CSF, no functional assays could be performed investigating the direct pathophysiological relevance of KCNA2 IgG. Patient-derived recombinant monoclonal KCNA2 autoantibodies, which would markedly facilitate such functional investigations, are currently not available. Although the number of patients in our cohort far exceeds previous reports on KCNA2 autoimmunity, prospective analysis of many further patients is needed for robust clinical-pathological correlations and treatment recommendations.

## Conclusion

Regardless of future studies investigating the possible causal or secondary role of KCNA2 autoantibodies in humans, we suggest that – already now – immunotherapy should be considered in patients with KCNA2 autoantibodies, especially if the autoantibodies occur in CSF and if the clinical phenotype consists of autoimmune encephalitis, atypical dementia, new-onset epilepsy and unexplained epileptic seizures. Treatment should be administered as early as possible if diagnostic findings suggest ongoing inflammation and may include steroids, plasma exchange, IVIG, therapeutic apheresis, and B cell depletion.

## Funding

This work was supported by grants from the German Research Foundation (DFG; grants FOR3004, PR1274/3–1, PR1274/5–1, and PR1274/9–1), by the Helmholtz Association (HIL-A03 BaoBab), and by the German Federal Ministry of Education and Research (Connect-Generate 01GM1908D) to HP.

M.E. received funding from DFG under Germanýs Excellence Strategy – EXC-2049 – 390,688,087, Collaborative Research Center ReTune TRR 295—424778381, BMBF, DZNE, DZHK, EU, Corona Foundation, and Fondation Leducq.

Open Access funding enabled and organized by Project DEAL.

## CRediT authorship contribution statement

**Friederike A. Arlt:** Conceptualization, Investigation, Methodology, Writing – original draft, Writing – review & editing. **Ramona Miske:** Formal analysis, Investigation, Methodology, Visualization, Writing – review & editing. **Marie-Luise Machule:** Investigation, Writing – review & editing. **Peter Broegger Christensen:** Investigation, Writing – review & editing. **Swantje Mindorf:** Investigation, Writing – review & editing. **Bianca Teegen:** Investigation, Writing – review & editing. **Kathrin Borowski:** Investigation. **Maria Buthut:** Investigation, Writing – review & editing. **Rosa Rößling:** Investigation, Writing – review & editing. **Elisa Sánchez-Sendín:** Investigation, Writing – review & editing. **Scott van Hoof:** Investigation, Writing – review & editing. **César Cordero-Gómez:** Investigation, Writing – review & editing. **Isabel Bünger:** Investigation, Writing – review & editing. **Helena Radbruch:** Investigation, Writing – review & editing. **Andrea Kraft:** Investigation, Writing – review & editing. **Ilya Ayzenberg:** Investigation, Writing – review & editing. **Jaqueline Klausewitz:** Investigation, Writing – review & editing. **Niels Hansen:** Investigation, Writing – review & editing. **Charles Timäus:** Investigation, Writing – review & editing. **Peter Körtvelyessy:** Investigation, Writing – review & editing. **Thomas Postert:** Investigation, Writing – review & editing. **Kirsten Baur-Seack:** Investigation, Writing – review & editing. **Constanze Rost:** Investigation, Writing – review & editing. **Robert Brunkhorst:** Investigation, Writing – review & editing. **Kathrin Doppler:** Investigation. **Niklas Haigis:** Investigation. **Gerhard Hamann:** Investigation, Writing – review & editing. **Albrecht Kunze:** Investigation, Writing – review & editing. **Alexandra Stützer:** Investigation, Writing – review & editing. **Matthias Maschke:** Investigation, Writing – review & editing. **Nico Melzer:** Investigation, Writing – review & editing. **Felix Rosenow:** Investigation, Writing – review & editing. **Kai Siebenbrodt:** Investigation, Writing – review & editing. **Christian Stenør:** Investigation, Writing – review & editing. **Martin Dichgans:** Investigation, Writing – review & editing. **Marios K. Georgakis:** Investigation, Writing – review & editing. **Rong Fang:** Investigation, Writing – review & editing. **Gabor C. Petzold:** Investigation, Writing – review & editing. **Michael Görtler:** Investigation, Writing – review & editing. **Inga Zerr:** Investigation, Writing – review & editing. **Silke Wunderlich:** Investigation, Writing – review & editing. **Ivan Mihaljevic:** Investigation, Writing – review & editing. **Paul Turko:** Investigation, Writing – review & editing. **Marianne Schmidt Ettrup:** Investigation, Writing – review & editing. **Emilie Buchholz:** Investigation, Writing – review & editing. **Helle Foverskov Rasmussen:** Investigation, Writing – review & editing. **Mahoor Nasouti:** Investigation, Writing – review & editing. **Ivan Talucci:** Investigation, Writing – review & editing. **Hans M. Maric:** Investigation, Writing – review & editing. **Stefan H. Heinemann:** Investigation, Writing – review & editing. **Matthias Endres:** Investigation, Writing – review & editing. **Lars Komorowski:** Investigation, Writing – review & editing. **Harald Prüss:** Conceptualization, Formal analysis, Methodology, Supervision, Writing – original draft.

## Declaration of Competing Interest

R.M., S.M., and L.K. are employes of EUROIMMUN.

## Data availability

Data will be made available on request.

## Acknowledgements

The authors would like to thank Petra Loge and Sonja Blumenau for excellent technical work.

## Appendix A. Supplementary data

Supplementary data to this article can be found online at https://doi.org/10.1016/j.bbi.2024.01.220.

## References


Barber, P.A., Anderson, N.E., Vincent, A., 2000. Morvan's syndrome associated with voltage-gated K+ channel antibodies. Neur. 54, 771–772. https://doi.org/10.1212/wnl.54.3.771.

Barthel, P.C., Staabs, F., Li, L.Y., Buthut, M., Otto, C., Ruprecht, K., Prüss, H., Höltje, M., 2023. Immunoreactivity to astrocytes in different forms of dementia: High prevalence of autoantibodies to GFAP. Brain Behav. Immun. Health 29, 100609. https://doi.org/10.1016/j.bbih.2023.100609.

Buckley, C., Oger, J., Clover, L., Tüzün, E., Carpenter, K., Jackson, M., Vincent, A., 2001. Potassium channel antibodies in two patients with reversible limbic encephalitis. Ann. Neurol. 50, 73–78. https://doi.org/10.1002/ana.1097.

Bünger, I., Makridis, K.L., Kreye, J., Nikolaus, M., Sedlin, E., Ullrich, T., Hoffmann, C., Tromm, J.V., Rasmussen, H.F., Milovanovic, D., Höltje, M., Prüss, H., Kaindl, A.M., 2023. Maternal synapsin autoantibodies are associated with neurodevelopmental delay. Front. Immunol. 14, 1101087. https://doi.org/10.3389/fimmu.2023.1101087.

Corbett, M.A., Bellows, S.T., Li, M., Carroll, R., Micallef, S., Carvill, G.L., Myers, C.T., Howell, K.B., Maljevic, S., Lerche, H., Gazina, E.V., Mefford, H.C., Bahlo, M., Berkovic, S.F., Petrou, S., Scheffer, I.E., Gecz, J., 2016. Dominant KCNA2 mutation causes episodic ataxia and pharmacoresponsive epilepsy. Neur. 87, 1975–1984. https://doi.org/10.1212/WNL.0000000000003309.

Daguano Gastaldi, V., Bh Wilke, J., Weidinger, C.A., Walter, C., Barnkothe, N., Teegen, B., Luessi, F., Stöcker, W., Lühder, F., Begemann, M., Zipp, F., Nave, K.-A., Ehrenreich, H., 2023. Factors predisposing to humoral autoimmunity against brain-antigens in health and disease: Analysis of 49 autoantibodies in over 7000 subjects. Brain Behav. Immun. 108, 135–147. https://doi.org/10.1016/j.bbi.2022.10.016.

Döring, J.H., Schröter, J., Jüngling, J., Biskup, S., Klotz, K.A., Bast, T., Dietel, T., Korenke, G.C., Christoph, S., Brennenstuhl, H., Rubboli, G., Møller, R.S., Lesca, G., Chaix, Y., Kölker, S., Hoffmann, G.F., Lemke, J.R., Syrbe, S., 2021. Refining genotypes and phenotypes in KCNA2-Related neurological disorders. Int. J. Mol. Sci. 22 https://doi.org/10.3390/ijms22062824.

Dubey, D., Hinson, S.R., Jolliffe, E.A., Zekeridou, A., Flanagan, E.P., Pittock, S.J., Basal, E., Drubach, D.A., Lachance, D.H., Lennon, V.A., McKeon, A., 2018. Autoimmune GFAP astrocytopathy: prospective evaluation of 90 patients in 1 year. J. Neuroimmunol. 321, 157–163. https://doi.org/10.1016/j.jneuroim.2018.04.016.

Fang, B., McKeon, A., Hinson, S.R., Kryzer, T.J., Pittock, S.J., Aksamit, A.J., Lennon, V. A., 2016. Autoimmune glial fibrillary acidic protein astrocytopathy: a novel meningoencephalomyelitis. JAMA Neurol. 73, 1297–1307. https://doi.org/10.1001/jamaneurol.2016.2549.

Flanagan, E.P., McKeon, A., Lennon, V.A., Boeve, B.F., Trenerry, M.R., Tan, K.M., Drubach, D.A., Josephs, K.A., Britton, J.W., Mandrekar, J.N., Lowe, V., Parisi, J.E., Pittock, S.J., 2010. Autoimmune dementia: clinical course and predictors of immunotherapy response. Mayo Clin. Proc. 85, 881–897. https://doi.org/10.4065/mcp.2010.0326.

Flanagan, E.P., Hinson, S.R., Lennon, V.A., Fang, B., Aksamit, A.J., Morris, P.P., Basal, E., Honorat, J.A., Alfugham, N.B., Linnoila, J.J., Weinshenker, B.G., Pittock, S.J., McKeon, A., 2017. Glial fibrillary acidic protein immunoglobulin G as biomarker of autoimmune astrocytopathy: analysis of 102 patients. Ann. Neurol. 81, 298–309. https://doi.org/10.1002/ana.24881.

Gelpi, E., Höftberger, R., Graus, F., Ling, H., Holton, J.L., Dawson, T., Popovic, M., Pretnar-Oblak, J., Högl, B., Schmutzhard, E., Poewe, W., Ricken, G., Santamaria, J., Dalmau, J., Budka, H., Revesz, T., Kovacs, G.G., 2016. Neuropathological criteria of anti-IgLON5-related tauopathy. Acta Neuropathol. 132, 531–543. https://doi.org/10.1007/s00401-016-1591-8.

Giannoccaro, M.P., Gastaldi, M., Rizzo, G., Jacobson, L., Vacchiano, V., Perini, G., Capellari, S., Franciotta, D., Costa, A., Liguori, R., Vincent, A., 2021. Antibodies to neuronal surface antigens in patients with a clinical diagnosis of neurodegenerative disorder. Brain Behav. Immun. 96, 106–112. https://doi.org/10.1016/j.bbi.2021.05.017.

Grüter, T., Möllers, F.E., Tietz, A., Dargvainiene, J., Melzer, N., Heidbreder, A., Strippel, C., Kraft, A., Höftberger, R., Schöberl, F., Thaler, F.S., Wickel, J., Chung, H.-Y., Seifert, F., Tschernatsch, M., Nagel, M., Lewerenz, J., Jarius, S., Wildemann, B.C., de Azevedo, L., Heidenreich, F., Heusgen, R., Hofstadt-van Oy, U., Linsa, A., Maaß, J.J., Menge, T., Ringelstein, M., Pedrosa, D.J., Schill, J., Seifert-Held, T., Seitz, C., Tonner, S., Urbanek, C., Zittel, S., Markewitz, R., Korporal-Kuhnke, M., Schmitter, T., Finke, C., Brüggemann, N., Bien, C.I., Kleiter, I., Gold, R., Wandinger, K.-P., Kuhlenbäumer, G., Leypoldt, F., Ayzenberg, I., German Network for Research on Autoimmune Encephalitis (GENERATE), 2023. Clinical, serological and genetic predictors of response to immunotherapy in anti-IgLON5 disease. Brain 146, 600–611. 10.1093/brain/awac090.

Guan, D., Lee, J.C.F., Higgs, M.H., Spain, W.J., Foehring, R.C., 2007. Functional roles of Kv1 channels in neocortical pyramidal neurons. J. Neurophysiol. 97, 1931–1940. https://doi.org/10.1152/jn.00933.2006.

Guan, D., Armstrong, W.E., Foehring, R.C., 2013. Kv2 channels regulate firing rate in pyramidal neurons from rat sensorimotor cortex. J. Physiol. 591, 4807–4825. https://doi.org/10.1113/jphysiol.2013.257253.

Ik, H., C, W., A, V., C, N., D, B., O, P., C, M., J, N.-D., 1997. Autoantibodies detected to expressed K+ channels are implicated in neuromyotonia. Annals of neurology 41. 10.1002/ana.410410215.

Irani, S.R., Alexander, S., Waters, P., Kleopa, K.A., Pettingill, P., Zuliani, L., Peles, E., Buckley, C., Lang, B., Vincent, A., 2010. Antibodies to Kv1 potassium channel-complex proteins leucine-rich, glioma inactivated 1 protein and contactin-associated protein-2 in limbic encephalitis, morvan's syndrome and acquired neuromyotonia. Brain 133, 2734–2748. https://doi.org/10.1093/brain/awq213.

Jan, L.Y., Jan, Y.N., 2012. Voltage-gated potassium channels and the diversity of electrical signalling. J. Physiol. 590, 2591–2599. https://doi.org/10.1113/jphysiol.2011.224212.

Johnston, J., Forsythe, I.D., Kopp-Scheinpflug, C., 2010. Going native: voltage-gated potassium channels controlling neuronal excitability. J. Physiol. 588, 3187–3200. https://doi.org/10.1113/jphysiol.2010.191973.

Kirschstein, T., Sadkiewicz, E., Hund-Göschel, G., Becker, J., Guli, X., Müller, S., Rohde, M., Hübner, D.-C., Brehme, H., Kolbaske, S., Porath, K., Sellmann, T., Großmann, A., Wittstock, M., Syrbe, S., Storch, A., Köhling, R., 2020. Stereotactically Injected Kv1.2 and CASPR2 Antisera Cause Differential Effects on CA1 Synaptic and Cellular Excitability, but Both Enhance the Vulnerability to Pro-epileptic Conditions. Front Synaptic Neurosci 12, 13. 10.3389/fnsyn.2020.00013.

Kreye, J., Wenke, N.K., Chayka, M., Leubner, J., Murugan, R., Maier, N., Jurek, B., Ly, L.-T., Brandl, D., Rost, B.R., Stumpf, A., Schulz, P., Radbruch, H., Hauser, A.E., Pache, F., Meisel, A., Harms, L., Paul, F., Dirnagl, U., Garner, C., Schmitz, D., Wardemann, H., Prüss, H., 2016. Human cerebrospinal fluid monoclonal N-methyl-D-aspartate receptor autoantibodies are sufficient for encephalitis pathogenesis. Brain 139, 2641–2652. https://doi.org/10.1093/brain/aww208.

Kunchok, A., Zekeridou, A., McKeon, A., 2019. Autoimmune glial fibrillary acidic protein astrocytopathy. Curr. Opin. Neurol. 32, 452–458. https://doi.org/10.1097/WCO.0000000000000676.

Lai, M., Huijbers, M.G.M., Lancaster, E., Graus, F., Bataller, L., Balice-Gordon, R., Cowell, J.K., Dalmau, J., 2010. Investigation of LGI1 as the antigen in limbic encephalitis previously attributed to potassium channels: a case series. Lancet Neurol. 9, 776–785. https://doi.org/10.1016/S1474-4422(10)70137-X.

Landa, J., Gaig, C., Plagumà, J., Saiz, A., Antonell, A., Sanchez-Valle, R., Dalmau, J., Graus, F., Sabater, L., 2020. Effects of IgLON5 Antibodies on Neuronal Cytoskeleton: A Link between Autoimmunity and Neurodegeneration. Ann. Neurol. 88, 1023–1027. https://doi.org/10.1002/ana.25857.

Lang, B., Makuch, M., Moloney, T., Dettmann, I., Mindorf, S., Probst, C., Stoecker, W., Buckley, C., Newton, C.R., Leite, M.I., Maddison, P., Komorowski, L., Adcock, J., Vincent, A., Waters, P., Irani, S.R., 2017. Intracellular and non-neuronal targets of voltage-gated potassium channel complex antibodies. J. Neurol. Neurosurg. Psychiatry 88, 353–361. https://doi.org/10.1136/jnnp-2016-314758.

Long, Y., Liang, J., Xu, H., Huang, Q., Yang, J., Gao, C., Qiu, W., Lin, S., Chen, X., 2018. Autoimmune glial fibrillary acidic protein astrocytopathy in Chinese patients: a retrospective study. Eur. J. Neurol. 25, 477–483. https://doi.org/10.1111/ene.13531.

Manole, A., Männikkö, R., Hanna, M.G., 2017. SYNAPS study group, Kullmann, D.M., Houlden, H. De novo KCNA2 mutations cause hereditary spastic paraplegia. Ann. Neurol. 81, 326–328. https://doi.org/10.1002/ana.24866.

Masnada, S., Hedrich, U.B.S., Gardella, E., Schubert, J., Kaiwar, C., Klee, E.W., Lanpher, B.C., Gavrilova, R.H., Synofzik, M., Bast, T., Gorman, K., King, M.D., Allen, N.M., Conroy, J., Ben Zeev, B., Tzadok, M., Korff, C., Dubois, F., Ramsey, K., Narayanan, V., Serratosa, J.M., Giraldez, B.G., Helbig, I., Marsh, E., O'Brien, M., Bergqvist, C.A., Binelli, A., Porter, B., Zaeyen, E., Horovitz, D.D., Wolff, M., Marjanovic, D., Caglayan, H.S., Arslan, M., Pena, S.D.J., Sisodiya, S.M., Balestrini, S., Syrbe, S., Veggiotti, P., Lemke, J.R., Møller, R.S., Lerche, H., Rubboli, G., 2017. Clinical spectrum and genotype-phenotype associations of KCNA2-related encephalopathies. Brain 140, 2337–2354. https://doi.org/10.1093/brain/awx184.

McKeon, A., Shelly, S., Zivelonghi, C., Basal, E., Dubey, D., Flanagan, E., Madhavan, A.A., Mariotto, S., Toledano, M., Tracy, J.A., Zekeridou, A., Pittock, S.J., 2020. Neuronal intermediate filament IgGs in CSF: Autoimmune Axonopathy Biomarkers. Ann. Clin. Transl. Neurol. 8, 425–439. https://doi.org/10.1002/acn3.51284.

Miske, R., Scharf, M., Stark, P., Dietzel, H., Bien, C.I., Borchers, C., Kermer, P., Ott, A., Denno, Y., Rochow, N., Borowski, K., Finke, C., Teegen, B., Probst, C., Komorowski, L., 2021. Autoantibodies Against the Purkinje Cell Protein RGS8 in Paraneoplastic Cerebellar Syndrome. Neurol Neuroimmunol Neuroinflamm 8, e987.

Miske, R., Scharf, M., Borowski, K., Rieckhoff, N., Teegen, B., Denno, Y., Probst, C., Guthke, K., Didrihsone, I., Wildemann, B., Ruprecht, K., Komorowski, L., Jarius, S., 2023. Septin-3 autoimmunity in patients with paraneoplastic cerebellar ataxia. J. Neuroinflammation 20, 88. https://doi.org/10.1186/s12974-023-02718-9.

Prüss, H., 2021. Autoantibodies in neurological disease. Nat. Rev. Immunol. 1–16 https://doi.org/10.1038/s41577-021-00543-w.

Quek, A.M.L., Britton, J.W., McKeon, A., So, E., Lennon, V.A., Shin, C., Klein, C., Watson, R.E., Kotsenas, A.L., Lagerlund, T.D., Cascino, G.D., Worrell, G.A., Wirrell, E.C., Nickels, K.C., Aksamit, A.J., Noe, K.H., Pittock, S.J., 2012. Autoimmune epilepsy: clinical characteristics and response to immunotherapy. Arch. Neurol. 69, 582–593. https://doi.org/10.1001/archneurol.2011.2985.

Rocchi, A., Sacchetti, S., De Fusco, A., Giovedi, S., Parisi, B., Cesca, F., Höltje, M., Ruprecht, K., Ahnert-Hilger, G., Benfenati, F., 2019. Autoantibodies to synapsin I sequestrate synapsin I and alter synaptic function. Cell Death Dis. 10, 864. https://doi.org/10.1038/s41419-019-2106-z.

Scharf, M., Miske, R., Kade, S., Hahn, S., Denno, Y., Begemann, N., Rochow, N., Radzimski, C., Brakopp, S., Probst, C., Teegen, B., Stöcker, W., Komorowski, L., 2018. A Spectrum of Neural Autoantigens, Newly Identified by Histo-Immunoprecipitation, Mass Spectrometry, and Recombinant Cell-Based Indirect Immunofluorescence. Front. Immunol. 9, 1447. https://doi.org/10.3389/fimmu.2018.01447.

Shillito, P., Molenaar, P.C., Vincent, A., Leys, K., Zheng, W., van den Berg, R.J., Plomp, J. J., van Kempen, G.T., Chauplannaz, G., Wintzen, A.R., 1995. Acquired neuromyotonia: evidence for autoantibodies directed against K+ channels of peripheral nerves. Ann. Neurol. 38, 714–722. https://doi.org/10.1002/ana.410380505.

Timäus, C., von Gottberg, P., Hirschel, S., Lange, C., Wiltfang, J., Hansen, N., 2021. KCNA2 Autoimmunity in Progressive Cognitive Impairment: Case Series and Literature Review. Brain Sci. 11 https://doi.org/10.3390/brainsci11010089.

Titulaer, M.J., McCracken, L., Gabilondo, I., Armangué, T., Glaser, C., Iizuka, T., Honig, L.S., Benseler, S.M., Kawachi, I., Martinez-Hernandez, E., Aguilar, E., Gresa-Arribas, N., Ryan-Florance, N., Torrents, A., Saiz, A., Rosenfeld, M.R., Balice-Gordon, R., Graus, F., Dalmau, J., 2013. Treatment and prognostic factors for long-term outcome in patients with anti-NMDA receptor encephalitis: an observational cohort study. Lancet Neurol. 12, 157–165. https://doi.org/10.1016/S1474-4422(12)70310-1.

Turko, P., Groberman, K., Browa, F., Cobb, S., Vida, I., 2019a. Differential Dependence of GABAergic and Glutamatergic Neurons on Glia for the Establishment of Synaptic Transmission. Cereb. Cortex 29, 1230–1243. https://doi.org/10.1093/cercor/bhy029.

Turko, P., Groberman, K., Kaiser, T., Yanagawa, Y., Vida, I., 2019b. Primary Cell Culture of Purified GABAergic or Glutamatergic Neurons Established through Fluorescence-activated Cell Sorting. J. Vis. Exp. https://doi.org/10.3791/58974.

van Sonderen, A., Schreurs, M.W.J., de Bruijn, M.A.A.M., Boukhrissi, S., Nagtzaam, M.M.P., Hulsenboom, E.S.P., Enting, R.H., Thijs, R.D., Wirtz, P.W., Sillevis Smitt, P.A.E., Titulaer, M.J., 2016. The relevance of VGKC positivity in the absence of LGI1 and Caspr2 antibodies. Neurology 86, 1692–1699. https://doi.org/10.1212/WNL.0000000000002637.

Vincent, A., Buckley, C., Schott, J.M., Baker, I., Dewar, B.-K., Detert, N., Clover, L., Parkinson, A., Bien, C.G., Omer, S., Lang, B., Rossor, M.N., Palace, J., 2004. Potassium channel antibody-associated encephalopathy: a potentially immunotherapy-responsive form of limbic encephalitis. Brain 127, 701–712. https://doi.org/10.1093/brain/awh077.

Yellen, G., 2002. The voltage-gated potassium channels and their relatives. Nature 419, 35–42. https://doi.org/10.1038/nature00978.